

UCRL-JC-130557

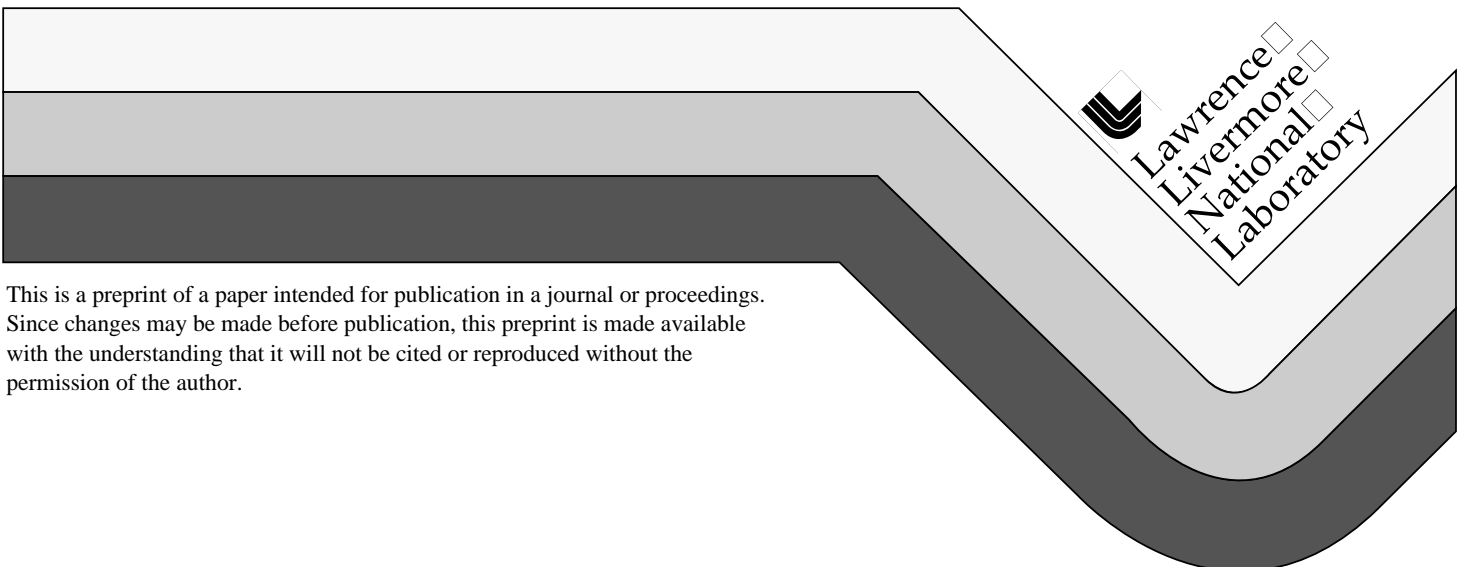
PREPRINT

Pressure Enhanced Penetration with Shaped Charge Perforators

L.A. Glenn

This paper was prepared for submittal to the
Eastern Regional Meeting of the Society of Petroleum Engineers
Pittsburgh, PA
November 9-13, 1998

May 18, 1998



This is a preprint of a paper intended for publication in a journal or proceedings.
Since changes may be made before publication, this preprint is made available
with the understanding that it will not be cited or reproduced without the
permission of the author.

DISCLAIMER

This document was prepared as an account of work sponsored by an agency of the United States Government. Neither the United States Government nor the University of California nor any of their employees, makes any warranty, express or implied, or assumes any legal liability or responsibility for the accuracy, completeness, or usefulness of any information, apparatus, product, or process disclosed, or represents that its use would not infringe privately owned rights. Reference herein to any specific commercial product, process, or service by trade name, trademark, manufacturer, or otherwise, does not necessarily constitute or imply its endorsement, recommendation, or favoring by the United States Government or the University of California. The views and opinions of authors expressed herein do not necessarily state or reflect those of the United States Government or the University of California, and shall not be used for advertising or product endorsement purposes.

**Pressure Enhanced Penetration
with
Shaped Charge Perforators**

L. A. Glenn
Computational Physics Group
Geophysics & Global Security Division
Lawrence Livermore National Laboratory

UCRL-JC-130557
May 18, 1998

Abstract

Computational analysis demonstrates that the penetration of a shaped charge jet can be enhanced by at least 25% by imploding the liner in a high pressure light gas atmosphere. The gas pressure helps confine the jet on the axis of penetration in the latter stages of formation. A light gas, such as helium or hydrogen, is required in order to keep the gas density low enough so as not to inhibit liner collapse.

1.0 Background and Motivation

Modern shaped charges are widely used for both military and commercial applications. Although the main operation is remarkably similar in both applications, there are at least two significant differences in the devices actually employed. The first is cost. Military applications generally demand much higher performance and, in particular, high reproducibility. This, in turn, requires the liner to be forged and precision machined. The main commercial use is in oil or gas well stimulation, in which the jet from the shaped charge is employed to create a flow path from the reservoir to the wellbore. In this application, a large number of perforators is inserted into the wellbore in what is called a gun. Although there are three basic types of guns, perhaps the most common is the casing gun, which can be run into the well on a wireline or conveyed by tubing. The charges are contained in a steel tube, protected from impact and from the well fluids, and are arranged so that they face radially outward from the vertical axis of the carrier. In these devices, the liners are pressed using powder metal technology and are at least 2 orders of magnitude less expensive than those used in typical missile warheads.

The second factor that distinguishes commercial shaped charges from those used in weapons is standoff, i.e., the distance from the liner base to the target (usually measured in charge diameters). The penetrating effectiveness of a shaped charge jet is markedly enhanced by standoff. The reason for this is quite simple. Shaped charge jets normally are formed with a high axial velocity gradient, the tip moving at speeds of 6-10 km/s. The standoff distance allows the jet to stretch or elongate before encountering the target and, to first order, the depth of penetration is directly proportional to the length of the penetrator. There is an optimum standoff. If the distance to the target is too great, the penetration can be much less than if there were no standoff. This occurs because the jet can only stretch so much before breaking; once broken the particles are easily deflected by small perturbations and no longer produce a coherent, unidirectional penetrator. At optimal standoff, typically 6-8 charge diameters (CD), the penetration can be enhanced by 50% or more relative to that achieved with zero standoff. Commercial perforators, however, are rarely able to operate at more than 1 CD because they must fit inside the casing gun which, in turn, must fit inside the casing.

Our motivation for performing this study derived from a suggestion by P. Halleck [1] that the weight (and hence the cost) of the gun might be reduced if the pressure inside and out could be equalized. This suggestion was prompted by our remarking that in a calculation we had performed, the penetration into a concrete target appeared to be little affected when the (air) pressure

surrounding the perforator was increased from 0.1 to 10 MPa (14.5 to 1,450 psia). Since the gun needs to operate at the bottom of a well in which the hydrostatic pressure can be tens of MPa, the wall thickness must be sufficient to withstand these pressures without imploding. Equalizing the pressure would allow the wall thickness of the gun to be cut at least in half. Allowing the well fluids inside the gun would not do, however, because the high density of these fluids would inhibit collapse of the liners. Since air at 10 MPa has a density at least one order of magnitude below that of water or drilling mud, perhaps pressurizing the gun as it is lowered into the wellbore might achieve the desired result.

In what follows we describe the results of a computational study of the effect of ambient pressure on shaped charge performance. To keep matters relevant, we focus on a single (commercial) perforator the design of which was kindly supplied by J. Regalbuto of Halliburton Energy Services, Inc. Since the (composite) liner is a mixture of (mainly) metal powders, the first task was to characterize this material by devising a constitutive model. The model was then validated by comparing the calculated jet tip velocity with experimental data and the calculated penetration with measurements made in a well-characterized (6061-T6 aluminum alloy) target. Next, we describe the results of a series of calculations of penetration into standard (API RP43) concrete targets in which only the pressure surrounding the perforator was varied. Although concrete is not a perfect surrogate for reservoir rock, it is not altogether dissimilar and by this means we were able to compare the predicted penetration with data from experiments in which the ambient pressure was atmospheric. Finally, we exhibit the superior results that are predicted when the surrounding air is replaced by helium and we conclude by summarizing the main results and discussing their ramifications.

2.0 Liner Characterization

Figure 1 shows a “to-scale” profile cutaway of the OMNI conical shaped charge (CSC) perforator employed in the study; the upper half of the figure shows the initial computational grid employed (all calculations were performed in arbitrary Lagrange-Eulerian - ALE - mode). As indicated in the figure the outer base diameter of the steel tamper is 46 mm. The explosive charge weighs 22.7 g and consists of 98.5-99% RDX, with the remainder a wax filler. The liner consists of a mixture of tungsten (45.20% by weight), tin (11.05%), copper (43.19%), and graphite (0.53%) powders, together with a small (0.03%) amount of lubricating oil. According to mixture theory, the density of the fully compacted liner should be 11.19 g/cm³. Measurement of the actual density, using the method of Archimedes, yielded a value of 10.15 g/cm³ [2], so that an initial gas porosity of 0.0929 was inferred.

A Grüneisen equation of state for the fully compacted powder was derived by D. A. Young of our Laboratory; the resultant parameters were: $c_0 = 3.79$ km/s, $s = 1.592$, $\gamma_0 = 1.8$, and $b = 0.5$. Here, c_0 is the bulk sound speed, s is the slope of the shock Hugoniot (in shock velocity-particle velocity space), γ_0 is the initial Grüneisen parameter, and b is the first order volume correction to γ_0 .

All simulations described in this report were performed with the CALE hydrocode, developed at LLNL by R. Tipton [3]. The pore compaction treatment in this code follows closely the standard p - α formulation initially devised by

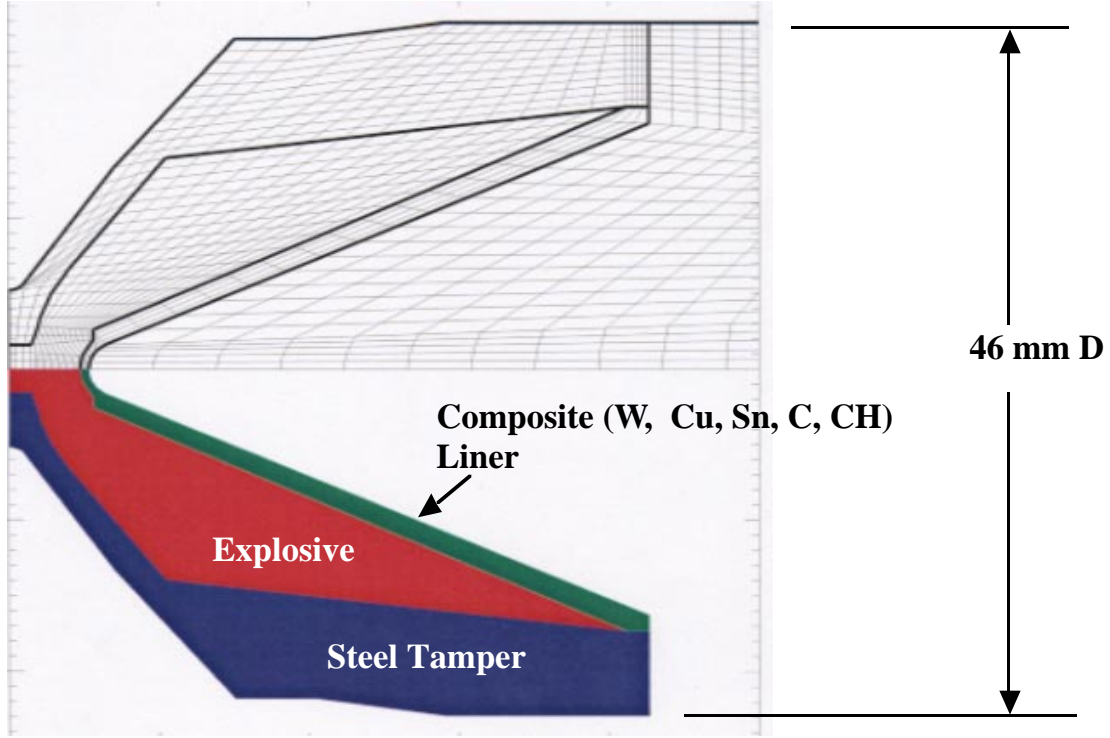


Fig. 1. Cross section of OMNI shaped charge perforator.

Carroll and Holt [4]. In our model, we prescribed a Hugoniot elastic limit of 50 MPa, with complete pore crushup occurring at 161 MPa. No independent measurements were made of the liner strength so that, in effect, the strength model constituted a degree of freedom available to help fit the penetration data. However, we found that employing the standard Steinberg-Guinan ductile failure model available in CALE, with parameters derived for copper, resulted in excellent agreement between predicted and measured jet tip velocity and in depth of penetration in (6061-T6) aluminum alloy targets; the experiments are described by Vigil [2].

Figure 2 shows the calculated penetration as a function of time, together with a snapshot crosssection at 10 μ s. The calculated jet tip velocity at this time was 6.4 km/s, the same value measured from the radiographs in the experiment. The final penetration was 265 mm, again in excellent agreement with the interpolated curve derived from the measurements (the calculation was performed at a standoff of 22.1 mm; the experiments were performed at standoffs of 6.35, 152.4, and 482.6 mm). The standoff position chosen for the calculations was the same as the position of the first target plate employed in the concrete penetration experiments, described below.

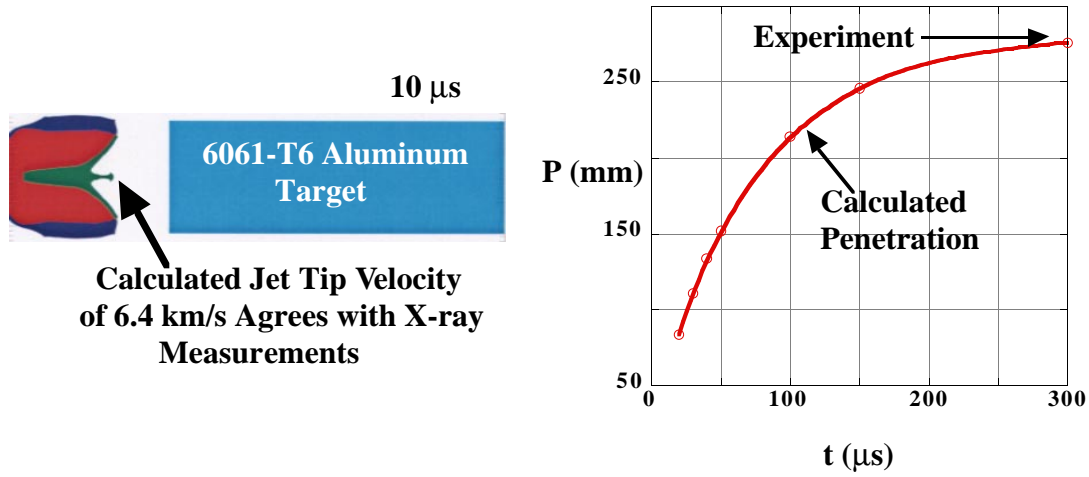


Fig. 2 Calculations of jet formation and penetration in a 6061-T6 aluminum alloy target are in good agreement with SNL measurements [2].

3.0 Concrete Penetration

Figure 3 illustrates the setup for the concrete penetration studies, which was chosen to replicate, as far as possible, the API Section 1 target. The outer boundary of the computational box was assumed rigid. The first steel target plate is supposed to simulate the gun wall and the second steel target plate butted up against the concrete is supposed to simulate the casing.

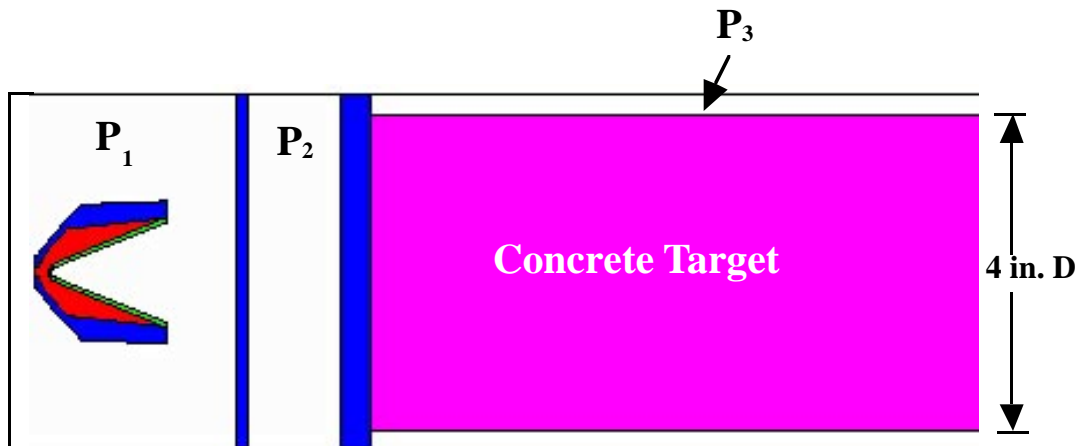


Fig. 3 Setup for concrete penetration studies. Gas pressure was independently variable in each of the 3 regions shown.

P_1 is the ambient pressure surrounding the perforator, P_2 is the pressure in the wellbore, and P_3 represents the reservoir pressure.

The concrete constitutive model employed is consistent with the specification for API RP43 Section1 targets and fits reasonably well the shock Hugoniot data reported for this material by Furnish [5]. The initial gas porosity was assumed to be 0.18, corresponding to a density of 2.15 g/cm³. The unconfined compressive strength was taken as 51.7 MPa (7,260 psi), and the strength increased with pressure up to a maximum of 160 MPa at a pressure of 1 GPa.

3.1 Penetration with Air as the Surrounding Gas

Figure 4 shows the results when the pressure P_1 is varied from 0.1 to 20 MPa (14.5 to 2,900 psia). The reservoir and wellbore pressures were assumed equal

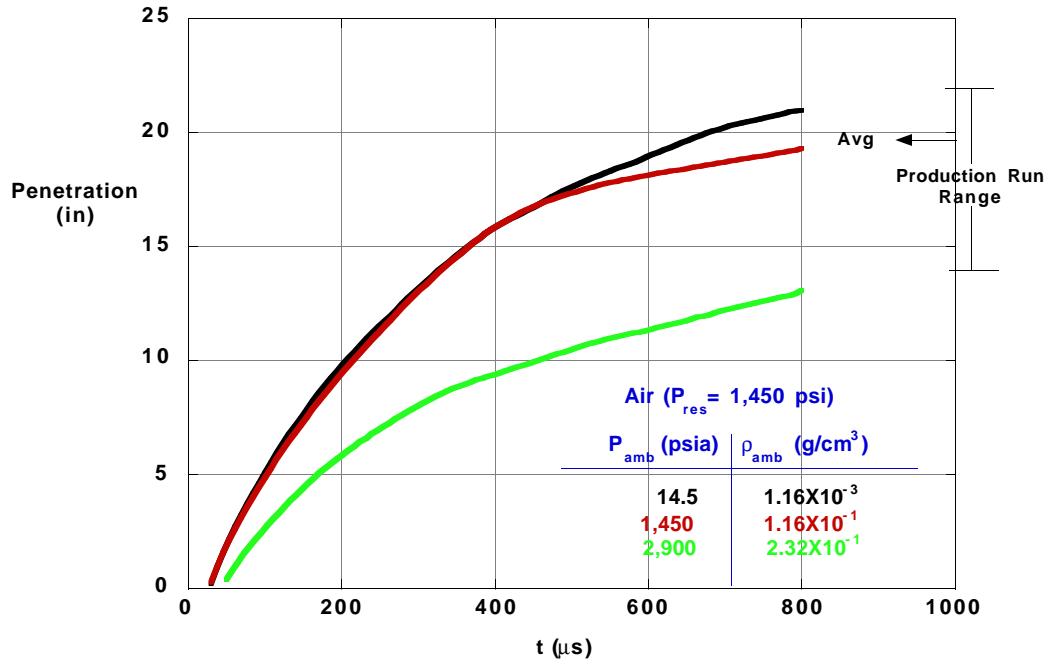


Fig. 4 Calculated penetration in concrete target as a function of ambient air pressure, P_1 . For these calculations, $P_2 = P_3 = 10$ MPa (1,450 psia).

and set to 1,450 psia (for consistency with industry practice, English units are used). It is observed that the penetration decreases monotonically with increasing ambient (gun) pressure, but that the final penetration is only about 8% less as P_1 increases from 0.01 to 10 MPa. The calculation with P_1 set to 14.5 psia is in reasonably good agreement with experimental data. According to Regalbuto [6], and as shown in Figure 4, the average penetration in this setup is 19.7 inches when the manufacturing process is under control. The measured range is from 14 to 22 inches during a production run.

As the pressure exceeds 1,450 psia, the penetration is seen to rapidly diminish. Figure 5 shows what happens when P_1 is increased from 2,900 to 4,350 psia.

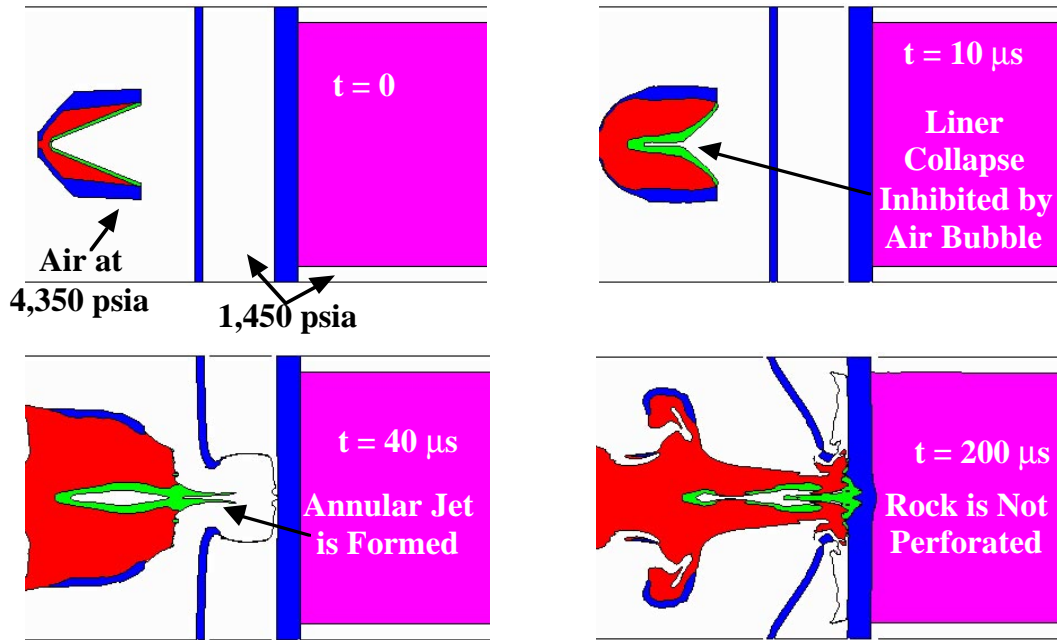


Fig. 5 Liner collapse process when the ambient air pressure, P_1 is set to 4,350 psia.

At $10 \mu s$, when the jet at low ambient air pressure is already well developed, no jet is observed; the liner collapse has been inhibited by the formation of a high-pressure air bubble. At $40 \mu s$, when the penetration in the concrete at low ambient air pressure is over 5 in., an annular jet has formed, and only the first steel plate has been perforated. At $200 \mu s$, the jet has completely broken up and even the steel casing has not been completely perforated.

Based on an analysis of these calculations, it was evident that the pressure acting on the jet was beneficial in that it helped confine the jet on the axis during the latter phase of formation. However, the increasing mass of the air inside the conical liner becomes more and more difficult to expel as the density is increased. Eventually, the density effect inhibits the formation of a stable jet altogether, as seen in the last frame in Figure 5.

3.1 Penetration with Helium as the Surrounding Gas

One way of improving the situation is to substitute a light gas, such as hydrogen or helium for the air. At the same pressure and temperature, the density is less by a factor of more than 14 with the former and 7 with the latter. The practical advantage of using an inert gas, however, probably outweighs the theoretical advantage of hydrogen and we have chosen this, more conservative, path in our subsequent analysis. Also, we increased the reservoir and wellbore pressure from 1,450 psia to 5,000 psia, which has the effect of increasing the strength of the concrete. Figure 6 shows the results of varying P_1 from 14.5 to 10,000 psia.

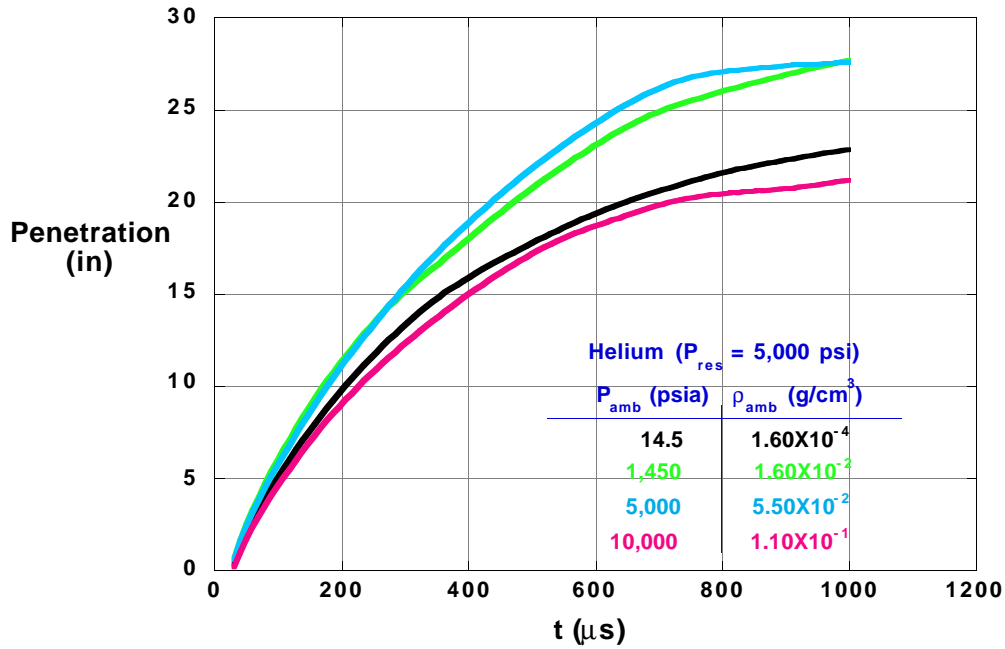


Fig. 6 Calculated penetration in concrete target as a function of ambient helium pressure, P_1 . For these calculations, $P_2 = P_3 = 34.5 \text{ MPa}$ (5,000 psia).

In this case, increasing the ambient pressure, P_1 , from 14.5 to 1450 psia substantially increases the penetration, and increasing P_1 by another factor of 3.4, to 5,000 psia, further increases the penetration. At still higher pressure, the penetration begins to decrease; when the initial surrounding helium pressure is 10,000 psia, the penetration is still slightly higher than that achieved with air at 1,450 psia; the gas density is about the same in these two cases.

It appears that the maximum penetration, with helium, occurs when P_1 is between 1,500 and 5,000 psia. Figure 7 crossplots the data in Figure 6. It is observed that, although final penetration has not stabilized in all the calculations, the penetration at 1,500 psia is at least 25% greater than obtained when the liner is surrounded by air at normal pressure.

Figures 8 and 9 illustrate the physical basis for this increased performance. In both figures, cross sections are overlaid of just the liner material for each of the calculations discussed in Figures 6 and 7. In Figure 8, the overlays are displayed at $10 \mu\text{s}$, when the jet tip velocity has attained its maximum value, prior to perforation of the first plate (gun wall). A yellow color is used for the 14.5 psia calculation. The color green is used to show the liner cross sections for each of the other calculations. It is clearly observed that, as the initial helium pressure surrounding the liner is increased, the base of the jet is forced to recede and an increasingly narrow and elongated jet is produced.

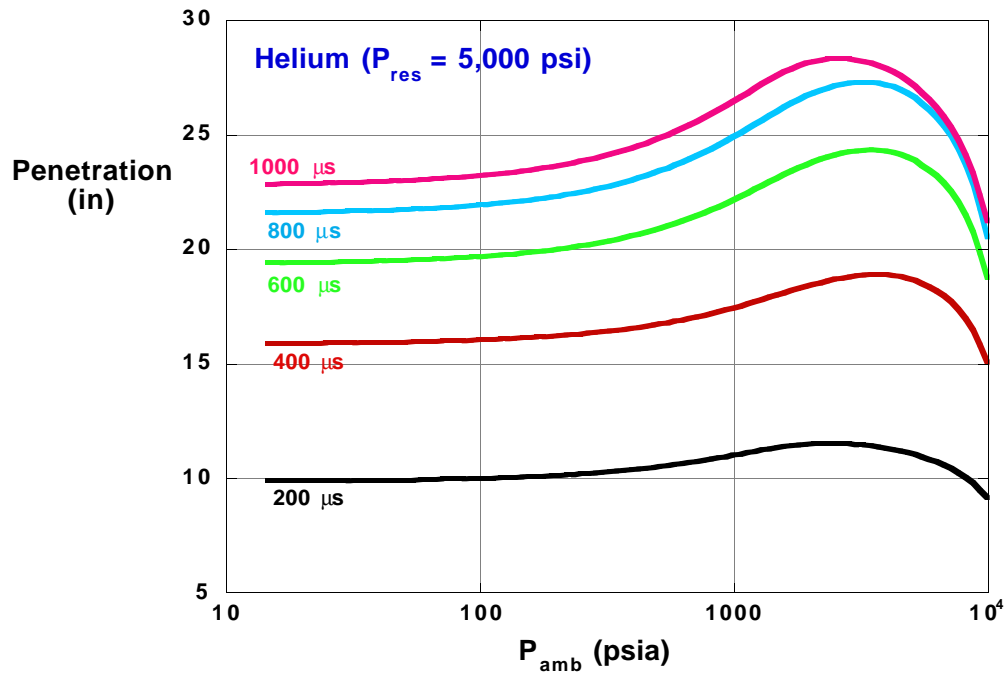


Fig. 7 Crossplot of the penetration data in Figure 6, showing maximum penetration occurring for $1,500 < P_1 < 5,000$ psia.

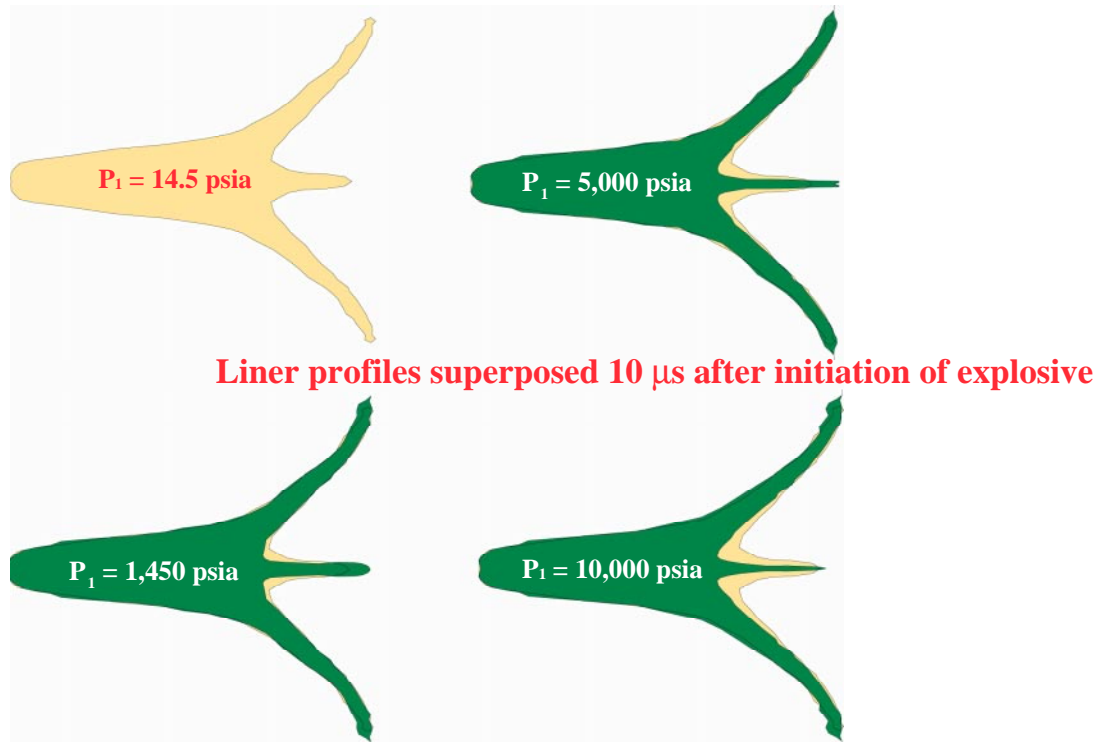
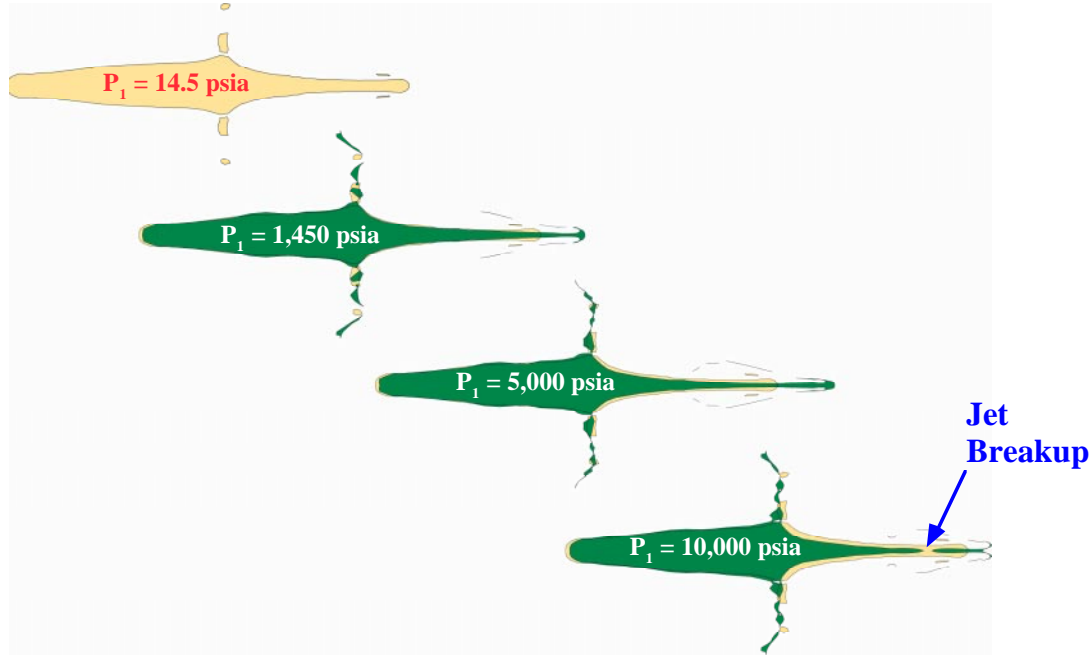


Fig. 8 Increasing the helium pressure surrounding the liner produces an increasingly narrow and elongated jet.



Liner profiles superposed 20 μ s after initiation of explosive

Fig. 9 Increasing the helium pressure surrounding the liner stretches the jet and increases penetration depth in the target until jet breakup occurs.

Figure 9 depicts the liner profiles at 20 μ s. As the initial surrounding pressure increases, the jets are seen to elongate and their cross sections diminish. When P_1 is 10,000 psia, the tip is still slightly ahead of the low-pressure case, but the calculation shows evidence of jet breakup beginning to occur. Although there is no explicit constitutive model for breakup in the code, the interface treatment implicitly produces this effect when the cross section gets sufficiently small; gas and jet material are then intermixed, and the local density is concomitantly reduced which, in turn, tends to decrease penetration.

4.0 Conclusions

Computational analysis of a commercial jet perforator has shown that the penetration can be substantially enhanced by imploding the liner in a high pressure, light gas atmosphere. With helium at 1,500 - 5,000 psia, the penetration into confined concrete cylinders was increased by at least 25% in comparison to that achieved when the liner was operated in air at standard temperature and pressure. The increased performance results from the gas pressure acting to confine the jet on the axis of penetration in the latter stages of formation. Since high density is concomitant with high pressure, a light gas, such as helium or hydrogen is required in order to keep the gas density low enough so as not to inhibit liner collapse.

Experimental verification of the results of this study has not yet been accomplished, but is planned in the near future.

Commercial perforators used in oil or gas well stimulation are normally disadvantaged by the short standoff forced upon them by their insertion in casing guns; there is simply not enough space available for the jets to stretch to optimum length. In this study, we have seen how high gas pressure helps to compensate for the lack of space by squeezing on the periphery of the jet, thereby producing added elongation. High pressure gas surrounding the perforator has the added advantage downhole that the wall thickness of the casing gun can be diminished, since the pressure differential between the internal gun and wellbore is thereby lessened. This has the potential for producing a lighter, and hence less costly, gun assembly. Balanced against these potential advantages is the added complexity in installing a high pressure system to go downhole. The system requires a pressure regulator that senses the exterior wellbore pressure and automatically adjusts the interior gun pressure to as to minimize the differential. An engineering cost benefit analysis is, however, beyond the scope of this study.

References

1. P. M. Halleck, personal communication, March 1998.
2. M. G. Vigil, *Conical Shaped Charge Pressed Powder, Metal Liner Jet Characterization and Penetration in Aluminum*, Sandia Report SAND97-1173, May 1997.
3. R. Tipton, *CALE Users Manual*, Lawrence Livermore National Laboratory Report 961101, November 1996.
4. M. M. Carroll and A. C. Holt, *J. Appl. Phys.*, **43**, 759-761 (1972).
5. M. Furnish, *Shock Properties of the API-43 Concrete and Castlegate Sandstone* (ACTI Near Wellbore Mechanics Project), Sandia National Laboratory Draft Technical Memorandum, 1997.
6. J. Regalbuto, personal communication, September 8, 1997.

Acknowledgement

This research was performed under the auspices of the U. S. Department of Energy by Lawrence Livermore National Laboratory under contract #W-7405-Eng-48. Budget support was provided by Mr. Roy Long (DOE/FETC). The author is grateful for useful discussions with Professor Phillip M. Halleck of the Petroleum and Natural Gas Engineering Department at the Pennsylvania State University and with Dr. John Regalbuto of Halliburton Energy Services Co.